# Self-assembly and properties of a discrete water-soluble *PrussianBlueAnalog* Fe$^{II}$/Co$^{III}$ cube; confinement of a water molecule in aqueous solution

*Miguel A. Gonzálvez, Albert Gallen, Montserrat Ferrer,[*] Manuel Martínez[*]*

Secció de Química Inorgànica, Departament de Química Inorgànica i Orgànica, Universitat de Barcelona. manel.martinez@qi.ub.edu montse.ferrer@qi.ub.es

**Supplementary Information**

## 1. Physical Methods

NMR spectra were recorded on a Varian Mercury-400 or Bruker-400Q spectrometers at 25 ºC ($^1$H 400 MHz or $^{13}$C 100.6 MHz) at the Unitat de RMN d´Alt Camp de la Universitat de Barcelona. DOSY NMR measurements were performed on a Bruker 400 MHz NMR spectrometer equipped with a 5 mm CPPBBO BB-1H/19F/D Z-GRD probe with a maximum strength of 5.5 G/mm at 298 K. The 90 pulse length was determined for sample. A standard LEDBPGP2S sequence was used with sinusoidal pulse field gradients and two spoiler gradients. A recovery delay of 150 μs and an LED delay of 5 ms were employed to reduce eddy current effects. The gradient strength was calibrated by using the self-diffusion coefficient of residual HOD in D$_2$O ($1.9 \times 10^{-9}$ m$^2$ s$^{-1}$). The gradient strength was increased from 2 – 95% in sixteen equally spaced steps with eight scans per increment. Values of δ (gradient pulse length) and Δ (diffusion time) were selected to give an intensity of about 5% of the initial intensity at 95% gradient strength. MNova software was used to process data.

ESI mass spectra were performed at the Unitat d'Espectrometria de Masses de Caracterització molecular dels Centres Científics i Tecnològics (Universitat de Barcelona) in a Agilent Technologies LC/MSD-TOF working in the negative mode spectrometer using H$_2$O-CH$_3$CN 1:1 to introduce the sample. ICP-OES was also carried out at the Centres Científics i Tecnològics (Universitat de Barcelona) on a Perkin Elmer Optima instrument. UV-Vis spectra were recorded on HP5483 or Cary50 instruments. IR spectra were recorded on a Thermo Scientific Nicolet iS5 FT-IR instrument using an ATR system.

Electrochemistry experiments were carried out at 25 ºC and at 100 mV s$^{-1}$, unless stated, with a BioLogic SP-150 instrument. A glassy carbon working electrode, a Ag/AgCl (saturated KCl) reference electrode and platinum wire counter electrode were used on $1 \times 10^{-3}$ M solutions of the

sample and using 0.1 M NaClO$_4$ (or KCl, depending of the cage) as supporting electrolyte. All potentials are given *versus* NHE, once corrected for the reference electrode used ($E^o$ Ag/AgCl/sat.KCl = +195 mV *versus* NHE).

p$K_a$ determination was carried out both by UV-Vis spectroscopy titrations using $2\times10^{-3}$ M solutions of the complex and adding small aliquots of 1 M HClO$_4$. Electronic spectra were recorded by using a Helma 661.202-UV All Quartz Immersion Probe connected to a Cary 50 instrument with optical fibres. The determination of the p$K_a$ values was carried out in this case using the standard Specfit or ReactLab Equilibrium software.[1,2]

The kinetic profiles for the reactions were followed by UV-Vis spectroscopy in the 900-300 nm range on a Cary50 instrument equipped with thermostated multicell transport. Observed rate constants were derived from absorbance versus time traces at the wavelengths where a maximum increase and/or decrease of absorbance were observed. The calculation of the observed rate constants from the absorbance *versus* time monitoring of reactions, studied under first order concentration conditions, were carried out using the SPECFIT or ReactLab software packages.[1,2] All post-run fittings were carried out by the standard available commercial programs.

Molecular modelling was carried out using SPARTAN (see reference 33 in the main text). DFT calculations were carried with the Spartan software using the B3LYP hybrid functional,[3-5] and LACVP as a basis set.[6]

## 2. Compounds

Compound [Co(Me$_3$-Tacn)Cl$_3$] was prepared according to literature methods.[7] Na$_4$[Fe$^{II}$(CN)$_6$] and K$_4$[Fe$^{II}$(CN)$_6$] were recrystallized twice from the commercially available material before use. All the other commercially available chemicals were of analytical grade and were used as received.

**Synthesis of Na$_4$[{Co$^{III}$(Me$_3$-Tacn)}$_4${Fe$^{II}$(CN)$_6$}$_4$]**

[Co(Me$_3$-Tacn)Cl$_3$] (0.24 g, 0.7 mmol) was dissolved in 100 mL of water, and the pH was adjusted to 8 with aqueous NaOH (the solution turns purple). Then, a solution of Na$_4$[Fe$^{II}$(CN)$_6$]·10H$_2$O (1 g, 2.1 mmol) in 30 mL of water was added dropwise, and the resulting green mixture was heated to 60 °C while stirred during 18 h. During the first hours of the reaction, the pH was carefully checked and adjusted when necessary. Thereafter, the obtained purple mixture was filtered, concentrated to a minimum volume and loaded onto a Sephadex G-25 M size exclusion column. After a first dark grey band, which is associated to an inorganic polymer, a second purple band, which contains the {Fe$^{II}$$_4$Co$^{III}$$_4$}$^{4-}$ box, was separated. The purple fraction was passed

through the column once again, diluted to 500 mL with 0.1 M $NaClO_4$ and loaded onto a Sephadex DEAE A-25 anion exchange column. The desired product starts to run through the column with 0.2 M $NaClO_4$ and is fully collected with 0.3 M $NaClO_4$. The eluate is then loaded again onto a Sephadex G-25 M whereof a major purple band was collected and taken to dryness at 40-50 ºC under vacuum. The solid obtained was extracted several times with MeOH in order to eliminate as much $NaClO_4$ as possible. Further concentration to dryness gave the desired product as a deep purple solid in 30% yield (based on metal concentrations).

$^1$H NMR (400 MHz, $D_2O$, 298 K) (δ/ppm): 2.91 (s, 36 H, $CH_3$), 3.04-3.16 (m, 24H, $CH_2$ *anti*), 3.29-3.41 (m, 24H, $CH_2$ *syn*), 3.87 (s, 2H, encapsulated $H_2O$).

$^{13}$C NMR (100.6 MHz, $D_2O$, 298 K) (δ/ppm): 51.8 (s, $CH_3$), 60.9 (s, $CH_2$), 169.4 (s, terminal C≡N), 182.0 (s, bridging C≡N).

MS-ESI(-) ($H_2O$:$CH_3CN$ 1:1) (m/z): 916.1130 $[[\{Co(Me_3\text{-Tacn})\}_4\{Fe(CN)_6\}_4]+2Na^++H_2O]^{2-}$; calcd: 916.1158; 907.1114 $[[\{Co(Me_3\text{-Tacn})\}_4\{Fe(CN)_6\}_4]+2Na^+]^{2-}$; calcd: 907.1105; 896.1178 $[[\{Co(Me_3\text{-Tacn})\}_4\{Fe(CN)_6\}_4]+Na^++H^+]^{2-}$; 896.1196; 603.0740 $[[\{Co(Me_3\text{-Tacn})\}_4\{Fe(CN)_6\}_4]+Na^++H_2O]^{2-}$; calcd: 603.0808; 597.0791 $[[\{Co(Me_3\text{-Tacn})\}_4\{Fe(CN)_6\}_4]+Na^+]^{3-}$; calcd: 597.0773.

UV-Vis ($H_2O$): {nm (ε /$M^{-1}$ $cm^{-1}$)}: 324 (2740), 457 (sh, 3820), 525 (4710).

IR (ATR) ($cm^{-1}$): 2148 m, 2123 s, 2055 vs, ν(C≡N).

ICP-OES: Ratio Fe-Co 1.01±0.01

## Synthesis of $K_4[\{Co^{III}(Me_3\text{-Tacn})\}_4\{Fe^{II}(CN)_6\}_4]$

The synthesis of the potassium derivative was carried out in analogous way to that described above for the sodium box. 1M KOH solution was used to adjust the pH to 8 when needed and 0.2-0.3 M KCl were used as eluent in the anion exchange chromatography (Sephadex DEAE A-25 anion column). From 0.24 g (0.7 mmol) $[Co(Me_3\text{-Tacn})Cl_3]$ and 0.88 g (2.1mmol) of $K_4[Fe^{II}(CN)_6]\cdot3H_2O$ the potassium box was obtained as a deep purple solid in 40% yield (based on metal concentrations).

$^1$H NMR (400 MHz, $D_2O$, 298 K): (δ/ppm) 2.93 (s, 36H, $CH_3$), 3.07-3.19 (m, 24H, $CH_2$ *anti*), 3.30-3.42 (m, 24H, $CH_2$ *syn*).

$^{13}$C NMR (100.6 MHz, $D_2O$, 298 K) (δ/ppm}: 52.0 (s, $CH_3$), 61.0 (s, $CH_2$), 169.1 (s, terminal C≡N), 181.00 (s, bridging C≡N).

MS-ESI(-) ($H_2O$:$CH_3CN$ 1:1) (m/z): 923.0828 $[[\{Co(Me_3\text{-Tacn})\}_4\{Fe(CN)_6\}_4]+2K^+]^{2-}$; calcd: 923.0850; 602.4012 $[[\{Co(Me_3\text{-Tacn})\}_4\{Fe(CN)_6\}_4]+K^+]^{3-}$; calcd: 602.4022;

UV-Vis ($H_2O$) {nm (ε /$M^{-1}$ $cm^{-1}$)}: 317 (2600), 455 (sh, 3950), 518 (4740).

IR (ATR) ($cm^{-1}$): 2151 m, 2125 s, 2063 vs, ν(C≡N).

ICP-OES: Ratio Fe-Co 1.03±0.02

**Description of the Spartan-DFT calculated structure**

The averaged Fe-Co distance derived from the theoretical calculations 4.93 Å, is a bit smaller than that described for closely related [8] cubes (see references 13, 15, 16 in the main manuscript). The dihedral angle Fe-Co-Fe-Co found for the square unit represented in figure S1b is 0.76°, very similar to those of the other faces of the optimised cube, a fact that confirms the planarity of all of them.

In this respect, several attempts to substitute the $[Na \cdot H_2O]^+$ ionic pair by $Cs^+$ or $NH_4^+$ at room temperature produced no changes on the NMR spectrum of the cubes. A fact that can be attributed to the particular dimensions of the $\{Fe_2Co_2\}$ square faces of this kinetically inert-structure cages.
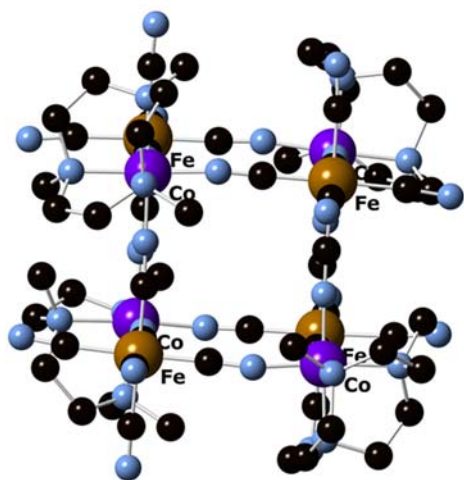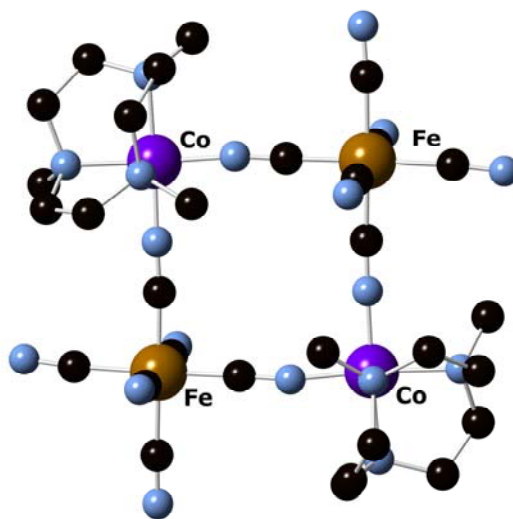
**Figure S1.** Representation of the Spartan-calculated structure (DFT-B3LYP) of the cubic cage $[\{Co^{III}(Me_3\text{-}Tacn)\}_4\{Fe^{II}(CN)_6\}_4]^{4-}$ (a) and one of the $\{\{Co^{III}(Me_3\text{-}Tacn)\}_2\{Fe^{II}(CN)_6\}_2\}$ units (b).

*a)*  *b)*
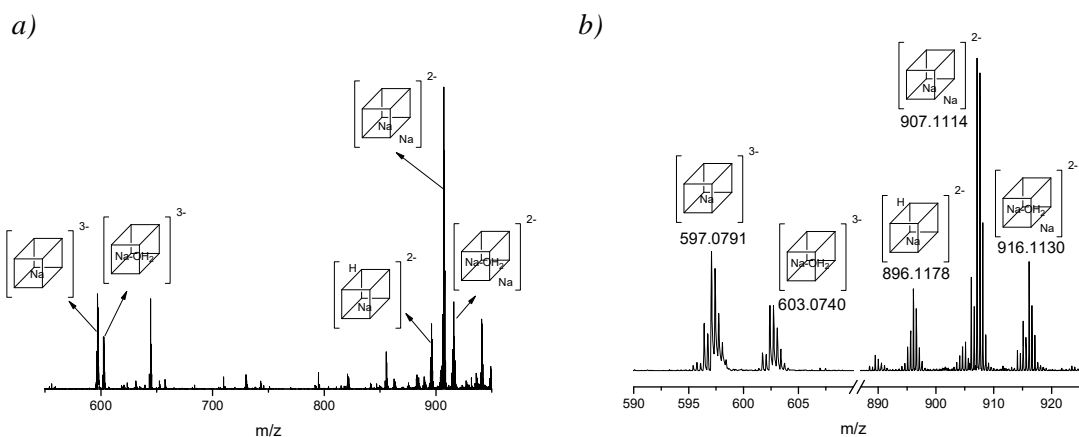


**Figure S2.** MS-ESI(-) (H$_2$O:CH$_3$CN 1:1) spectrum, *a)*, and relevant inset, *b)*, of the Na$_4$[{Co$^{III}$(Me$_3$-Tacn)}$_4${Fe$^{II}$(CN)$_6$}$_4$] derivative.

*a)*  *b)*
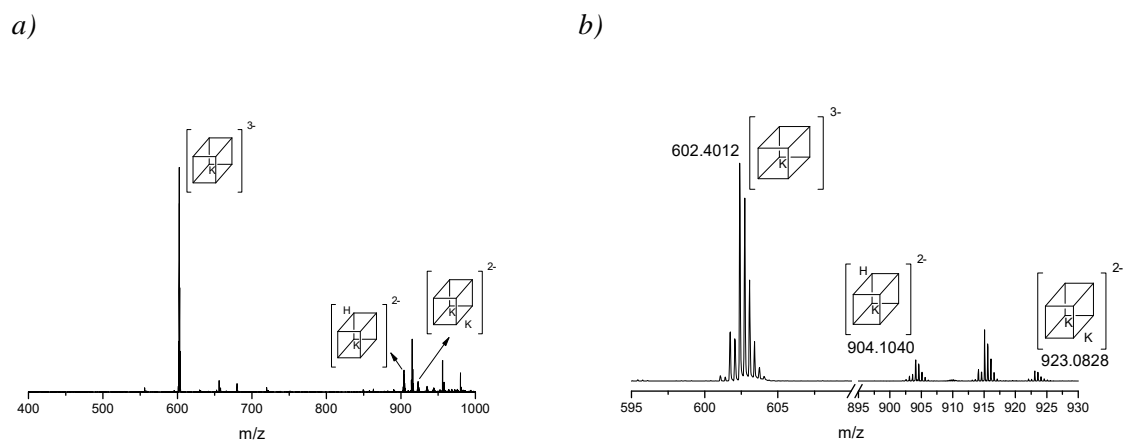


**Figure S3.** MS-ESI(-) (H$_2$O:CH$_3$CN 1:1) spectrum, *a)*, and relevant inset, *b)*, of the K$_4$[{Co$^{III}$(Me$_3$-Tacn)}$_4${Fe$^{II}$(CN)$_6$}$_4$] derivative.
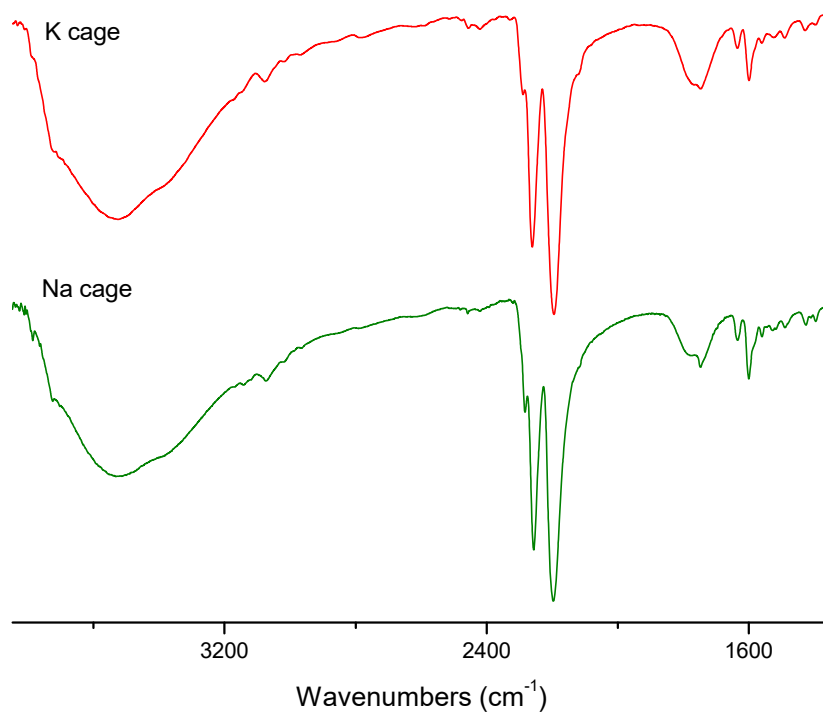
**Figure S4.** IR spectra of the $Na_4[\{Co^{III}(Me_3\text{-}Tacn)\}_4\{Fe^{II}(CN)_6\}_4]$ and $K_4[\{Co^{III}(Me_3\text{-}Tacn)\}_4\{Fe^{II}(CN)_6\}_4]$ cages.
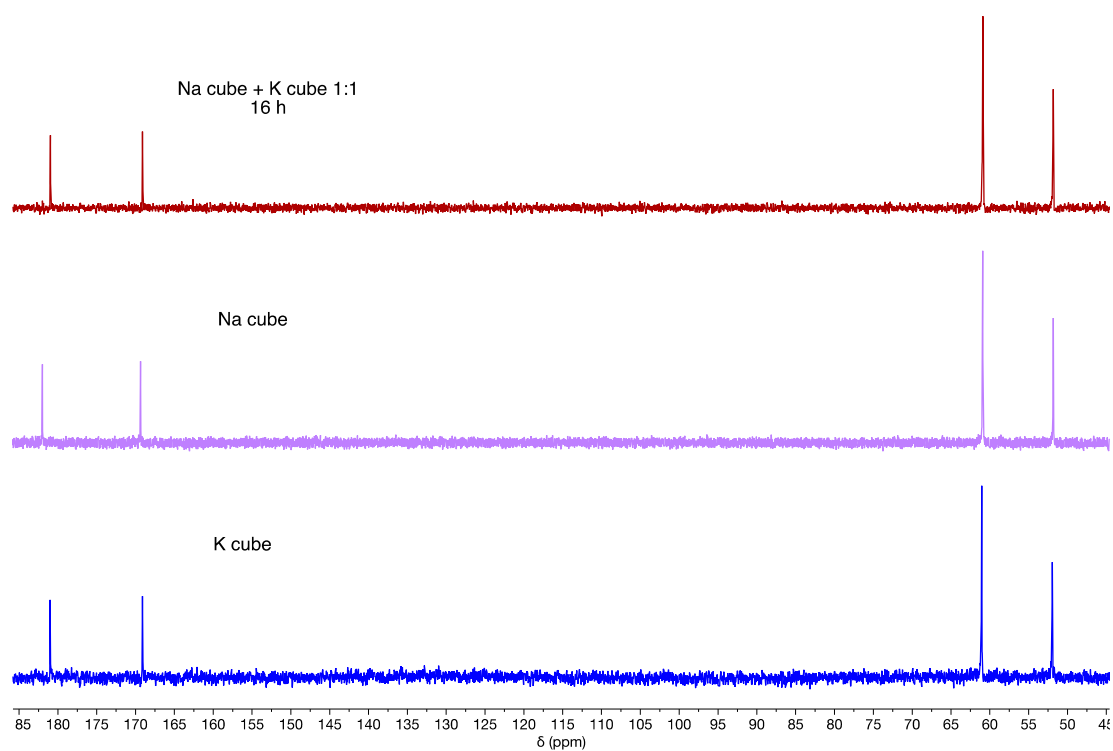
**Figure S5.** Comparison between the $^{13}$C NMR spectra of an equimolar mixture of Na$_4$[{Co$^{III}$(Me$_3$-Tacn)}$_4${Fe$^{II}$(CN)$_6$}$_4$] and K$_4$[{Co$^{III}$(Me$_3$-Tacn)}$_4${Fe$^{II}$(CN)$_6$}$_4$] and that of the corresponding sodium and potassium salts.
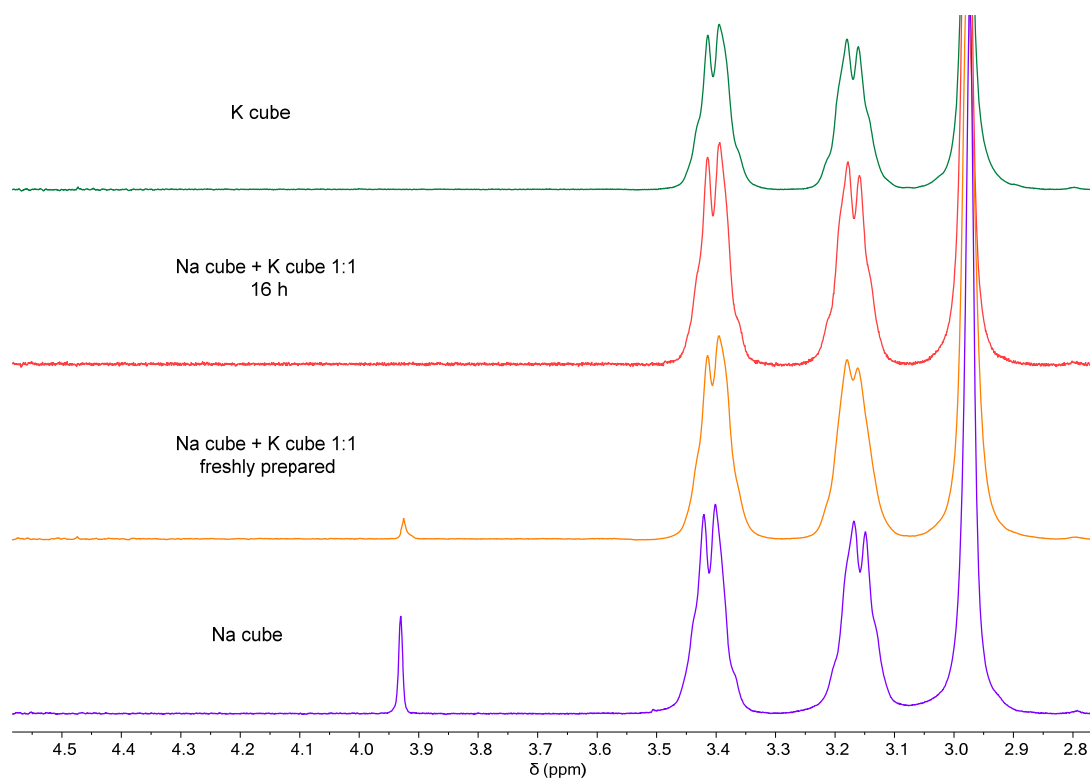
**Figure S6.** Comparison between the $^1H$ NMR spectra of an equimolar mixture of $Na_4[\{Co^{III}(Me_3\text{-}Tacn)\}_4\{Fe^{II}(CN)_6\}_4]$ and $K_4[\{Co^{III}(Me_3\text{-}Tacn)\}_4\{Fe^{II}(CN)_6\}_4]$ (at different times) and that of the corresponding sodium and potassium salts.
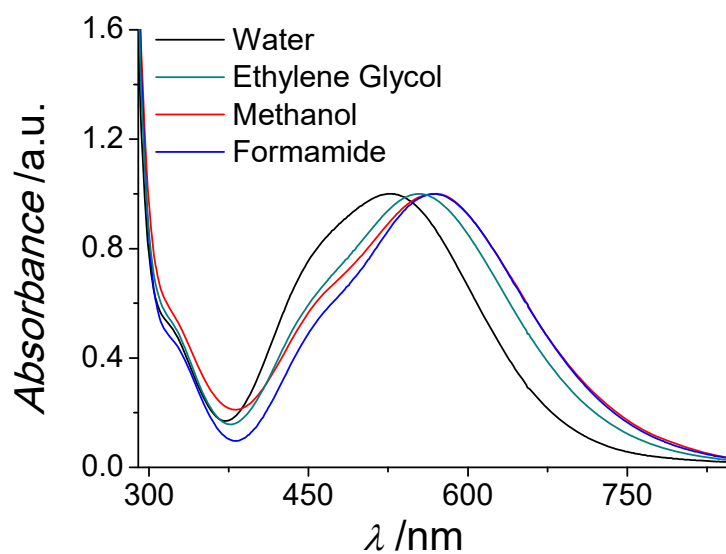
**Figure S7.** Solvatochromic shift observed for the MMCT band of the $Na_4[\{Co^{III}(Me_3-Tacn)\}_4\{Fe^{II}(CN)_6\}_4]$ cubic cage.

*a)#*

*b)*
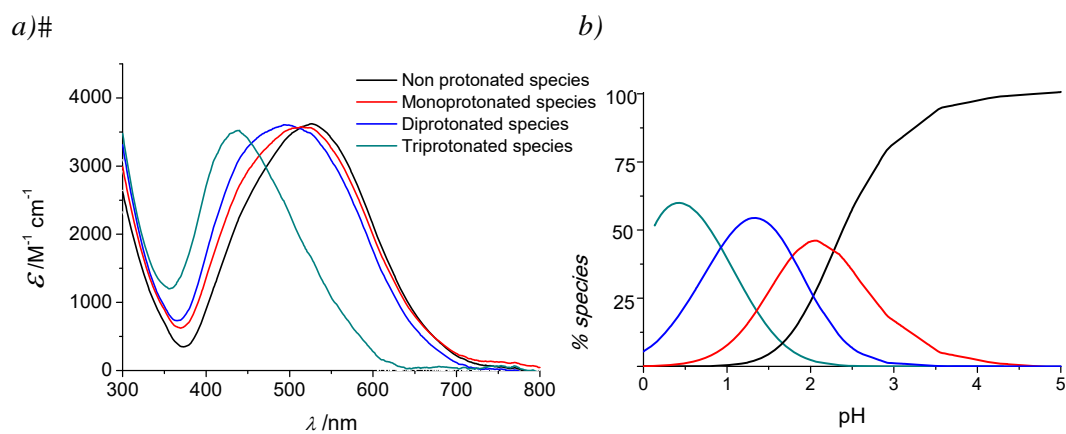


**Figure S8.-** a) Specfit-calculated spectra of the species present in solution according to the values determined for the p$K_a$ of $Na_4[\{Co^{III}(Me_3-Tacn)\}_4\{Fe^{II}(CN)_6\}_4]$. b) Speciation of the protonated species thus determined.
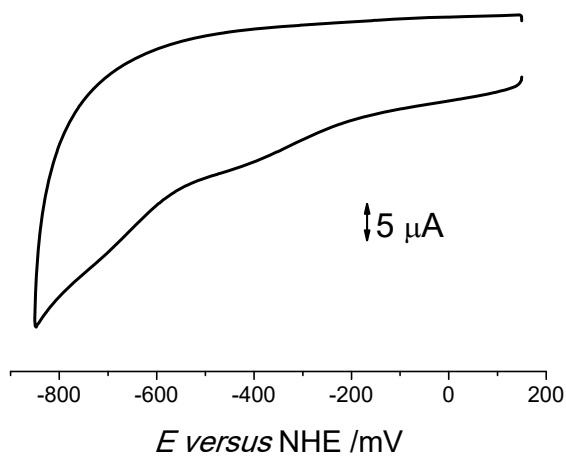
**Figure S9.** Cyclic voltammograms of the Co$^{III}$/Co$^{II}$ signals (WE: glassy carbon; AE: Pt wire; RE: Ag/AgCl(sat. KCl); 100 mV/s, 0.1 M NaClO$_4$, 25 ºC) of the Na$_4$[{Co$^{III}$(Me$_3$-Tacn)}$_4${Fe$^{II}$(CN)$_6$}$_4$] cage.
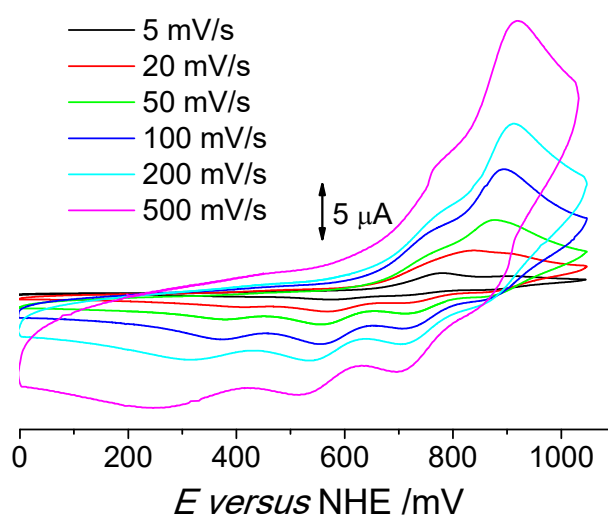


**Figure S10.** Cyclic voltammograms of the Fe$^{III}$/Fe$^{II}$ signals (WE: glassy carbon; AE: Pt wire; RE: Ag/AgCl(sat. KCl); 0.1 M NaClO$_4$, 25 ºC) at different scan rates of the sodium salt of the Na$_4$[{Co$^{III}$(Me$_3$-Tacn)}$_4${Fe$^{II}$(CN)$_6$}$_4$] cage prepared.
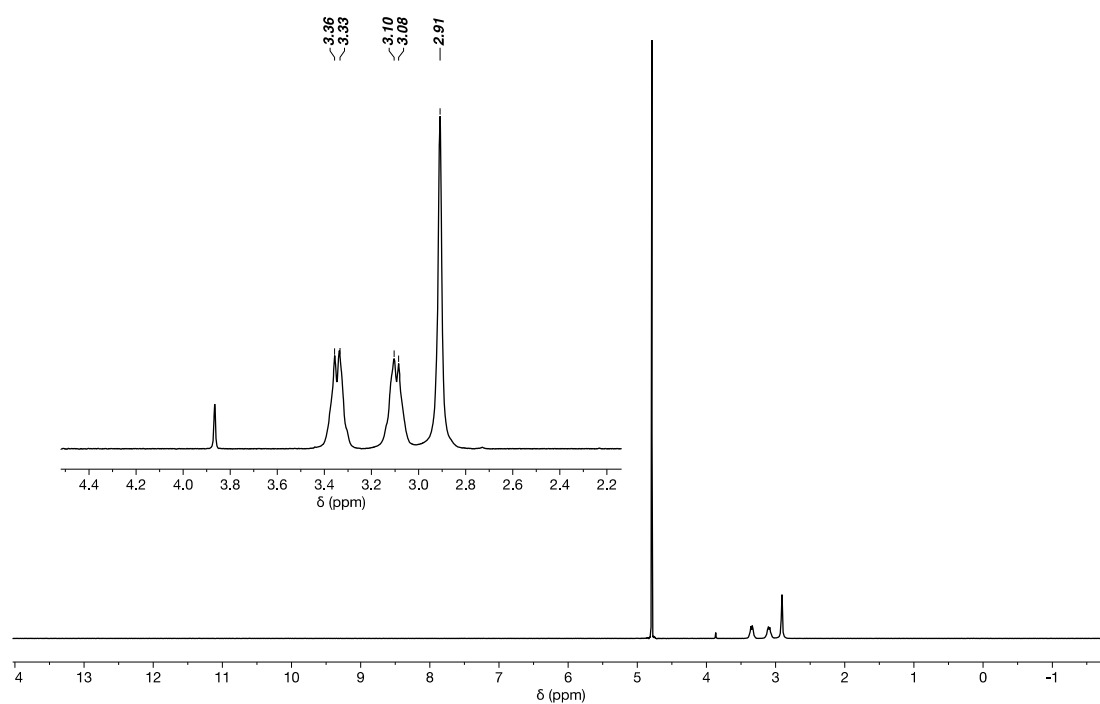
**Figure S11**. $^1$H NMR spectrum of Na$_4$[{Co(Me$_3$-Tacn)}$_4${Fe(CN)$_6$}$_4$] in D$_2$O at 298 K.
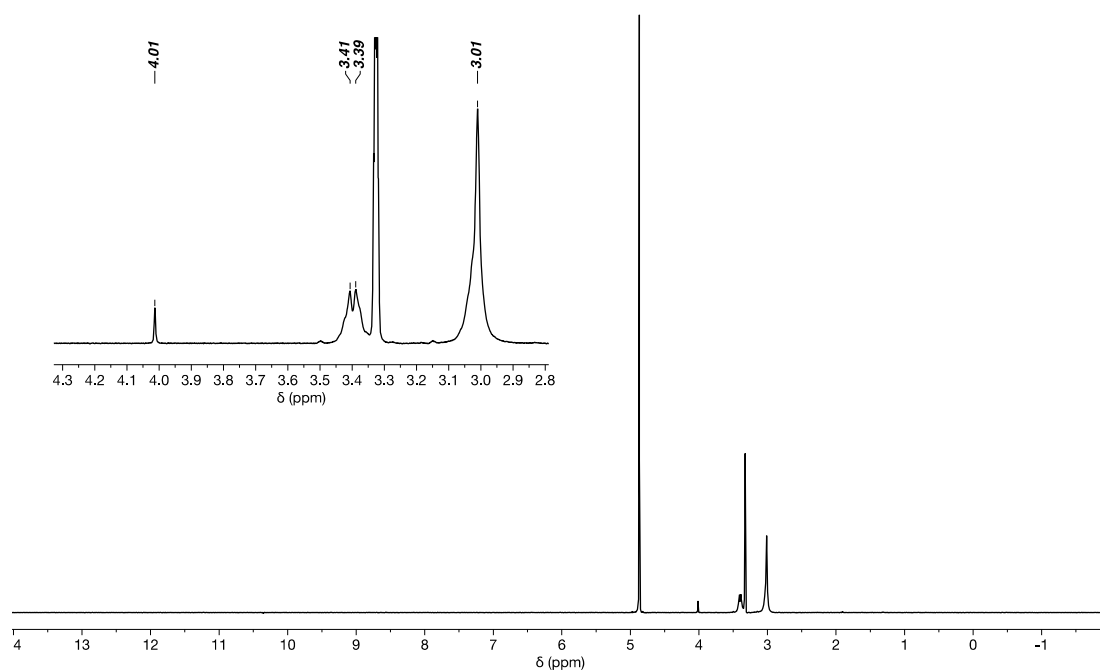


**Figure S12**. $^1$H NMR spectrum of Na$_4$[{Co(Me$_3$-Tacn)}$_4${Fe(CN)$_6$}$_4$] in Methanol-$d_4$ at 298 K.
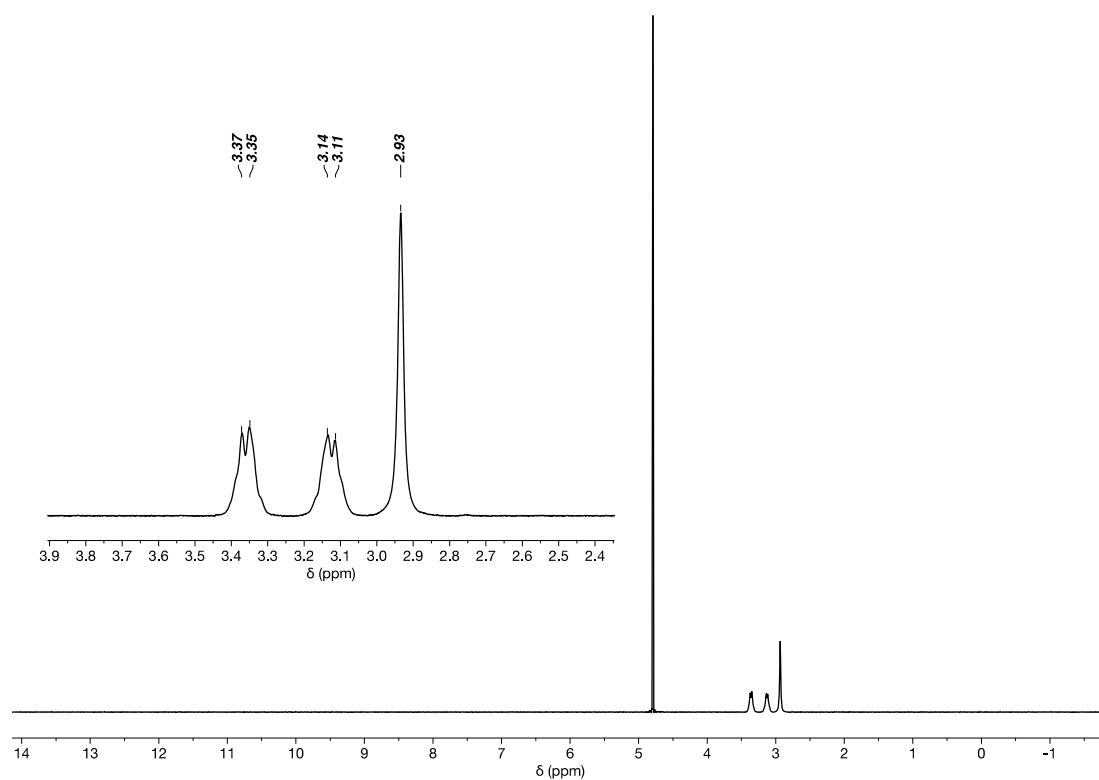
**Figure S13.** $^1$H NMR spectrum of K$_4$[{Co(Me$_3$-Tacn)}$_4${Fe(CN)$_6$}$_4$] in D$_2$O at 298 K.
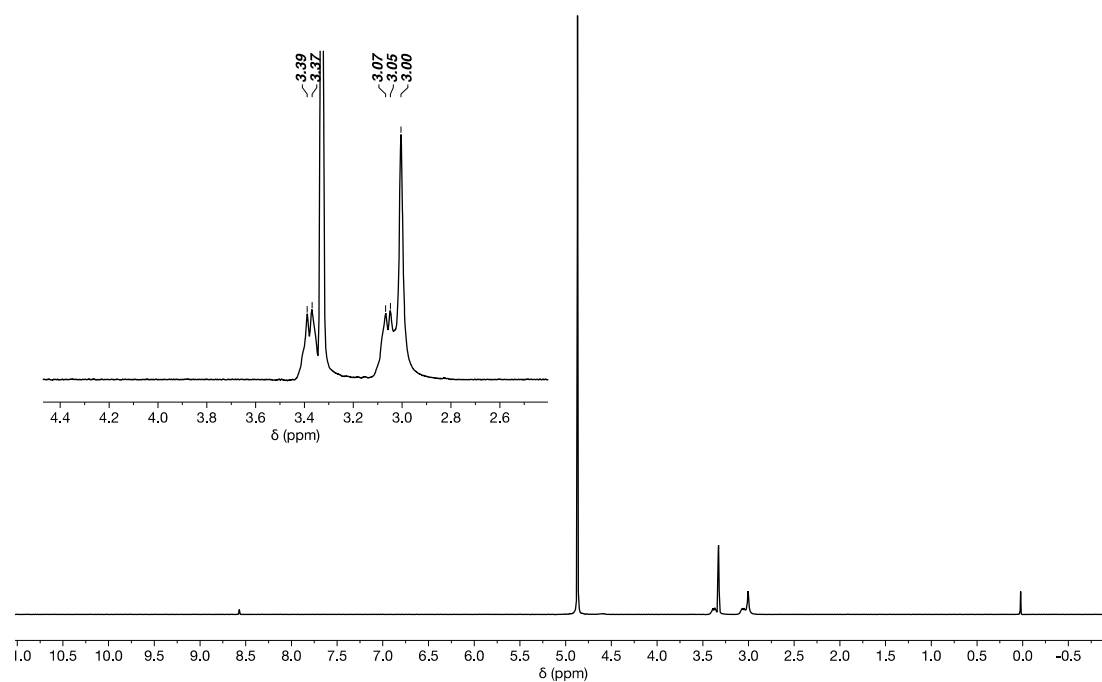


**Figure S14.** $^1$H NMR spectrum of K$_4$[{Co$^{III}$(Me$_3$-Tacn)}$_4${Fe$^{II}$(CN)$_6$}$_4$] in Methanol-$d_4$ at 298 K.
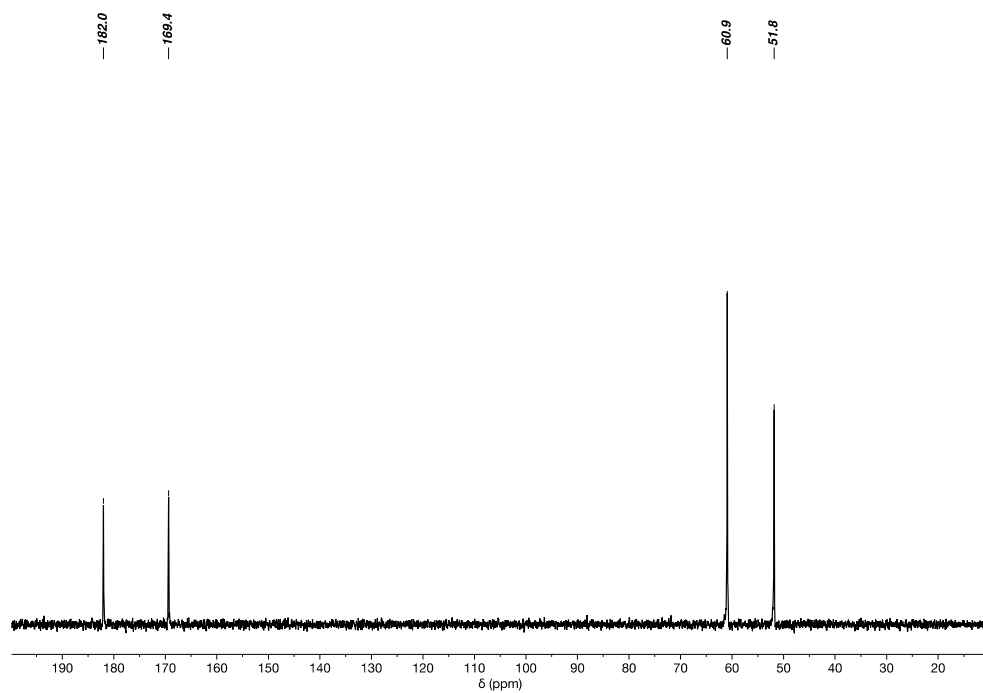
**Figure S15.** $^{13}$C NMR spectrum of Na$_4$[{Co$^{III}$(Me$_3$-Tacn)}$_4${Fe$^{II}$(CN)$_6$}$_4$] in D$_2$O at 298 K.
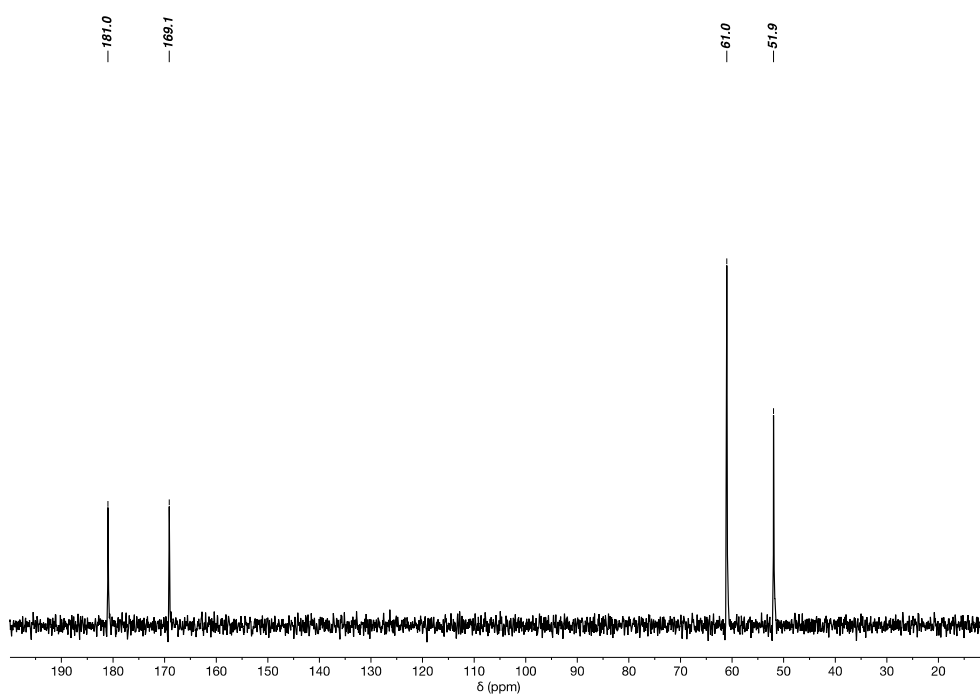


**Figure S16.** $^{13}$C NMR spectrum of K$_4$[{Co$^{III}$(Me$_3$-Tacn)}$_4${Fe$^{II}$(CN)$_6$}$_4$] in D$_2$O at 298 K.

**REFERENCES**

1.- *SPECFIT32,* version 3.0.34; Spectrum Software Associates: Marlborough, MA, USA, 2005

2.- *ReactLab,* Jplus Consulting Pty Ltd: East Fremantle, WA. Australia, 2009

3.- Hay, P. J.; Wadt, W. R. Ab initio effective core potentials for molecular calculations. Potentials for K to Au including the outermost core orbitals. *J. Chem. Phys.* **1985,** *82*, 299-310.

4.- Wadt, W. R.; Hay, P. J. Ab initio effective core potentials for molecular calculations. Potentials for main group elements Na to Bi. *J. Chem. Phys.* **1985,** *82*, 284-298.

5.- Becke, A. D. Density–functional thermochemistry. III. The role of exact exchange. *J. Chem. Phys.* **1993,** *98*, 5648-5652.

6.- Hehre, W. J.; Ditchfield, R.; Pople, J. A. Self–Consistent Molecular Orbital Methods. XII. Further Extensions of Gaussian–Type Basis Sets for Use in Molecular Orbital Studies of Organic Molecules. *J. Chem. Phys.* **1972,** *56*, 2257-2261.

7.- Searle, G. H.; Wang, D.-N.; Larsen, S.; Larsen, E. The Structure of a Novel Complex of Cobalt(III) with a Tridentate Macrocyclic Ligand with Tertiary Amine Donors, [CoL(NCCH3)2Cl]CoCl4 (L = 1,4,7-Trimethyl-1,4,7-triazacyclononane). *Acta. Chem. Scand.* **2019,** *46*, 38-42.

8.- Jiménez, J. R.; Tricoire, M.; Garnier, D.; Chamoreau, L. M.; von Bardeleben, J.; Journaux, Y.; Li, Y.; Lescouzec, R. A new {Fe4Co4} soluble switchable nanomagnet encapsulating Cs+: enhancing the stability and redox flexibility and tuning the photomagnetic effect. *Dalton Trans.* **2017,** *46*, 15549-15557.